Clim Dyn
DOI 10.1007/s00382-016-3003-0

The effect of future reduction in aerosol emissions on climate extremes in China

Zhili Wang[1] · Lei Lin[2] · Meilin Yang[3] · Yangyang Xu[4]

Received: 21 September 2015 / Accepted: 20 January 2016

Abstract This study investigates the effect of reduced aerosol emissions on projected temperature and precipitation extremes in China during 2031–2050 and 2081–2100 relative to present-day conditions using the daily data output from the Community Earth System Model ensemble simulations under the Representative Concentration Pathway (RCP) 8.5 with an applied aerosol reduction and RCP8.5 with fixed 2005 aerosol emissions (RCP8.5_FixA) scenarios. The reduced aerosol emissions of RCP8.5 magnify the warming effect due to greenhouse gases (GHG) and lead to significant increases in temperature extremes, such as the maximum of daily maximum temperature (TXx), minimum of daily minimum temperature (TNn), and tropical nights (TR), and precipitation extremes, such as the maximum 5-day precipitation amount, number of heavy precipitation days, and annual total precipitation from days $>$95th percentile, in China. The projected TXx, TNn, and TR averaged over China increase by 1.2 ± 0.2 °C (4.4 ± 0.2 °C), 1.3 ± 0.2 °C (4.8 ± 0.2 °C), and 8.2 ± 1.2 (30.9 ± 1.4) days, respectively, during 2031–2050 (2081–2100) under the RCP8.5_FixA scenario, whereas the corresponding values are 1.6 ± 0.1 °C (5.3 ± 0.2 °C), 1.8 ± 0.2 °C (5.6 ± 0.2 °C), and 11.9 ± 0.9 (38.4 ± 1.0) days under the RCP8.5 scenario. Nationally averaged increases in all of those extreme precipitation indices above due to the aerosol reduction account for more than 30 % of the extreme precipitation increases under the RCP8.5 scenario. Moreover, the aerosol reduction leads to decreases in frost days and consecutive dry days averaged over China. There are great regional differences in changes of climate extremes caused by the aerosol reduction. When normalized by global mean surface temperature changes, aerosols have larger effects on temperature and precipitation extremes over China than GHG.

Keywords Aerosols · RCP8.5 · Climate extremes

1 Introduction

Climate extremes (extreme weather or climate events) are defined as the occurrence of a weather or climate variable above (or below) a certain threshold value near the upper (or lower) ends of the range of observed values (IPCC 2012). There is a consensus that changes in the frequency or intensity of climate extremes significantly influence both human society and natural systems. Climate extremes can cause tremendous losses in life and economic activities (Easterling et al. 2000).

Climate extremes in many regions have changed in terms of the frequency and intensity during recent decades as the global surface temperature has experienced a marked increase (Zhai et al. 2005; Zhang et al. 2011). Some studies have found a detectable anthropogenic influence in the observed changes in frequency of extreme temperatures (e.g., Jones et al. 2008; Stott et al. 2011; Morak et al. 2012).

Zhili Wang and Lei Lin have contributed equally to this work.

✉ Zhili Wang
wangzl@camscma.cn

[1] State Key Laboratory of Severe Weather, Chinese Academy of Meteorological Sciences, Beijing 100081, China

[2] College of Atmospheric Sciences, Lanzhou University, Lanzhou 730000, China

[3] Beijing Meteorological Observation Center, Beijing 100089, China

[4] National Center for Atmospheric Research, Boulder, CO 80303, USA

Published online: 23 January 2016

Since the mid-20th century, anthropogenic forcing has very likely contributed to the observed changes in the frequency and intensity of daily temperature extremes at the global scale and has likely significantly increased the probability of occurrence of heat waves in some locations (Bindoff et al. 2013). Wen et al. (2013) indicated that anthropogenic influence was clearly detectable in Chinese extreme temperatures and the impact of greenhouse gases (GHG) may be the dominant contributor to the observed increase in extreme temperatures during 1961–2007. Sun et al. (2014) showed that anthropogenic influences, including GHG and aerosols, have led to a more than 60-fold increase in the likelihood of the extreme warm 2013 summer in eastern China since the early 1950s.

Many studies have projected changes in climate extremes under different emissions scenarios. A large number of global climate models (GCMs) have projected increases in climate extremes, such as extreme precipitation, consecutive dry days, and extremely hot days, under increased GHG concentrations and reduced aerosol emissions (e.g., Caesar and Lowe 2012; Kharin et al. 2013; Sillmann et al. 2013a; Zhou et al. 2014). Simulations for the twentyfirst century by a global climate model showed that many temperature-based indices, such as daily minimum temperature, daily maximum temperature, and the frequency of tropical nights (please see Sect. 2.3 about the definition), significantly increased worldwide (Sillmann and Roeckner 2008). Simulations by a regional climate model indicated that the number of frost days will decrease, and both the heat wave duration index and heavy precipitation will increase dramatically over China at the end of the twentyfirst century under the Representative Concentration Pathway (RCP) 8.5 scenario (Ji and Kang 2015). Mascioli et al. (2015) showed that the patterns of extreme temperature and precipitation associated with GHG forcing dominate in the U.S. during the twentyfirst century under the RCP8.5 scenario.

Aerosols are an important anthropogenic forcing agent, which can directly scatter or absorb sunlight (aerosol–radiation interaction) and alter cloud microphysical and radiative properties by acting as cloud condensation nuclei (CCN) or ice nuclei (aerosol–cloud interaction) (Boucher et al. 2013). Since the start of the industrial era, an increase in anthropogenic aerosol emissions has likely led to a net cooling of the Earth's climate system (Myhre et al. 2013). To mitigate environmental pollution and the resulting impacts on human health, governments worldwide will likely take continuous and stringent measures to reduce the emissions of most anthropogenic aerosols and their precursors during the twentyfirst century. This will result in gradual decreases in atmospheric aerosol concentrations and the net cooling effect of aerosols in the future (i.e., contributing to an additional warming) (Shindell et al. 2008; Wang et al. 2015a). Sillmann et al. (2013b) showed that future reduction in aerosol emissions could greatly enforce the warming effect due to GHG and increase the temperature and precipitation extremes in Europe. China is one of the most polluted regions in the world due to the rapid economic development experienced in recent decades. Aerosols have had a significant impact on regional climate change over China in the past (e.g., Zhang et al. 2012; Guo et al. 2013). However, the role that future reduction in aerosol emissions will play in projected climate extremes over China has not been investigated.

The objective of this study is to explore the effect of reduced aerosol emissions on projected near-term (2031–2050) and long-term (2081–2100) climate extremes over China under the RCP8.5 climate change scenario (a high GHG emission scenario) (Riahi et al. 2007), using daily data output from the simulations of a global climate model. Section 2 describes the model, simulations, and calculations of climate extremes. Section 3 presents the results. Finally, our discussion and conclusions are given in Sect. 4.

2 Model and methods

2.1 Model description

We used the Community Earth System Model (CESM1), which is a fully-coupled ocean–atmosphere–land–sea–ice model that can provide state-of-the-art simulations of the Earth's past, present, and future climate states (Hurrell et al. 2013). The horizontal resolution is 0.9° latitude × 1.25° longitude for the atmosphere and land, and 1° × 1° for the ocean. A comprehensive three-mode modal aerosol model (MAM3) that includes Aitken, accumulation, and coarse modes and two-moment bulk cloud microphysical scheme have been implemented in the model (Liu et al. 2012; Morrison and Gettelman 2008; Gettelman et al. 2010). MAM3 predicts the aerosol numbers and mass mixing ratios using internally mixed representations. The following assumptions are made for MAM3: (1) the primary carbon mode is merged with the accumulation mode, so that all primary carbon is internally mixed with secondary aerosol; (2) the coarse dust and sea salt modes are merged into a single coarse mode based on the assumption that the dust and sea salt are geographically separated; (3) the fine dust and sea salt modes are both merged with the accumulation mode; and (4) sulfate is partially neutralized by ammonium in the form of ammonium bisulfate, so ammonium is effectively prescribed and NH3 is not simulated. The total number of transported aerosol species is 15 (Liu et al. 2012). CESM1 contains the physics to represent aerosol direct effects, semi-direct effects, and indirect effects for both liquid and ice phase clouds (Ghan et al. 2012), and it is able to qualitatively

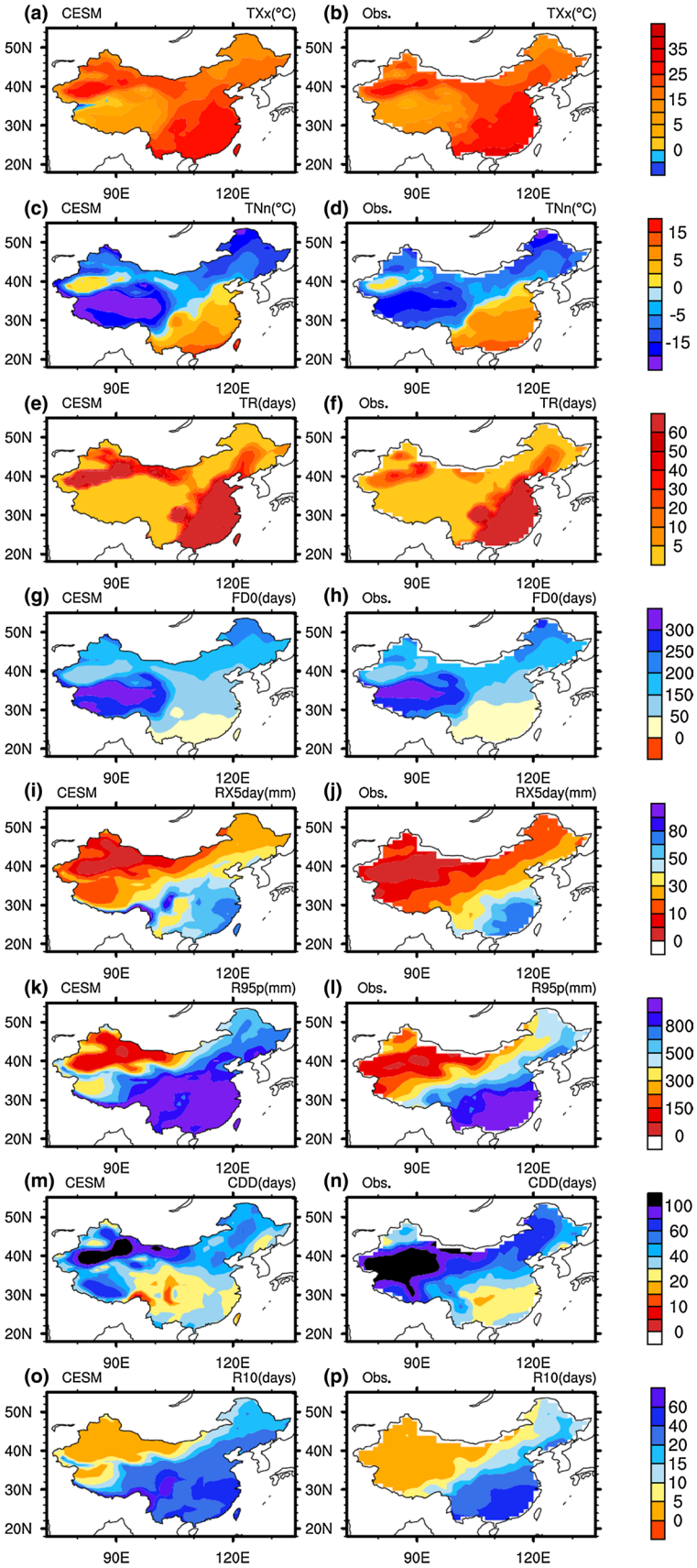

Fig. 1 The 1986–2005 time mean of climate extreme indices over China for CESM1 Large Ensemble simulations (*left column*) and gridded observations (*right column*)

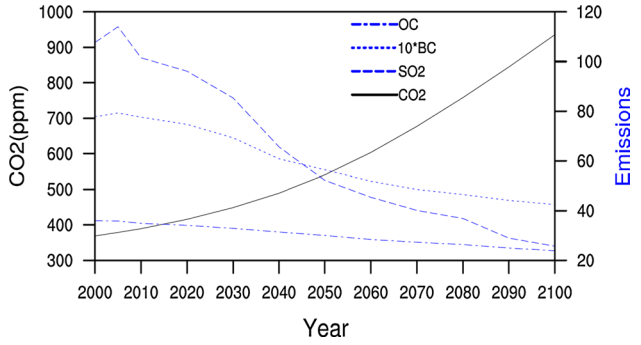

Fig. 2 Historical and RCP8.5 emissions for SO_2 (unit: Tg a^{-1}), BC and OC (units: TgC a^{-1}) and CO_2 concentration (unit: ppm) from 2000 to 2100

capture the observed geographical and temporal variations of aerosol mass and number concentrations, size distributions, and aerosol optical properties (Liu et al. 2012). The global annual mean aerosol direct, indirect, and total forcings from 1850 to 2000 simulated by the model are −0.02, −1.45, and −1.47 W m^{-2}, respectively (Ghan et al. 2012).

The historical climate extremes simulated by the CESM1 have been evaluated by Kharin et al. (2013), Fischer et al. (2013), Sillmann et al. (2013c), and Zhou et al. (2014). To show how well the CESM1 Large Ensemble simulations (see Sect. 2.2) represent present-day climate extremes over China, we compare the simulated results with the observational climate extremes data set during the period 1986–2005 (Fig. 1). The observation data are based on gridded daily precipitation and temperature at 1° × 1° resolution constructed from 2416 observation stations over China by the National Climate Center, China Meteorological Administration (Xu et al. 2009; Wu and Gao 2013). These results suggest that the model is able to capture the spatial distributions of climate extremes reasonably well.

2.2 Simulations

We used the daily data output from the CESM1 RCP8.5 Large Ensemble simulations (Kay et al. 2014) and RCP8.5 with fixed aerosols (RCP8.5_FixA) simulations (Xu et al. 2015). The RCP8.5 Large Ensemble consists of 30-member ensemble simulations from 1920 to 2100 under the RCP8.5 scenario. Each simulation uses the same trajectories of GHG and aerosol forcings, but starts from randomly perturbed initial conditions in the atmosphere. The RCP8.5_FixA ensemble consists of 15 members that use the same forcings as the RCP8.5 scenario except that all aerosol emissions and tropospheric oxidants are fixed at 2005 levels for the following years. Holding tropospheric oxidants fixed ensures that the production rate of sulfate from its precursor sulfur dioxide is unchanged. These simulations have been used to study terrestrial aridity under different scenarios (Lin et al. 2015) and the importance of aerosol scenarios in projections of future heat extremes (Xu et al. 2015). The RCP emissions scenarios are from Riahi et al. (2007). Figure 2 shows historical and RCP8.5 emissions for SO_2, BC, and OC, and the CO_2 concentration from 2000 to 2100. The estimated global annual mean radiative forcing by 2100 is 8.5 W m^{-2} under the RCP8.5 scenario relative to the pre-industry.

We examined the changes in projected climate extremes during 2031–2050 and 2081–2100 relative to the present-day conditions (2006–2015, henceforth PD) under the RCP8.5 and RCP8.5_FixA scenarios, respectively. The differences between the different periods under the RCP8.5 scenario were due to both changes in GHG and aerosol forcings, whereas under the RCP8.5_FixA scenario they were only due to change in GHG. We could then assess the contribution of reduced aerosol emissions on climate extremes in RCP8.5 by comparing the differences between the two scenarios.

2.3 Climate extremes indices

A set of indices based on daily temperature and precipitation data, as defined by the Expert Team for Climate Change Detection and Indices (ETCCDI) (Zhang et al. 2011), were used to explore the climate extremes. The maximum of daily maximum temperature (TXx) and minimum of daily minimum temperature (TNn) capture the hottest day and the coldest night temperature of the year, respectively. Tropical nights (TR) are defined as days with minimum temperatures above 20 °C, indicating very hot nighttime conditions. Higher nighttime temperatures can increase the heat stress for organisms (Sillmann and Roeckner 2008). Frost days (FD0) are defined as days with minimum temperatures less than 0 °C, indicating very cool conditions that have damaging effects on plant growths. The maximum 5-day precipitation amount (RX5 day) can be used as an indicator of flooding. The number of heavy precipitation days (R10) is the number of days with total precipitation more than 10 mm. Very wet days (R95p) describes the annual total precipitation from days more than 95th percentile. The same thresholds were used for all ensembles. Consecutive dry days (CDD) are defined as the maximum consecutive days with precipitation less than 1 mm, which is an indicator of drought.

Figure 3 shows the time series of changes in annual mean climate extreme indices averaged over China under the RCP8.5 and RCP8.5_FixA scenarios from 2006 to 2100 relative to the PD. The TXx, TNn, TR, RX5 day, R10, and R95p in China consistently increase, whereas the FD0 and CDD gradually decrease over time under both scenarios. There are few overlaps for the changes in these extreme indices in the future between both scenarios except the CDD.

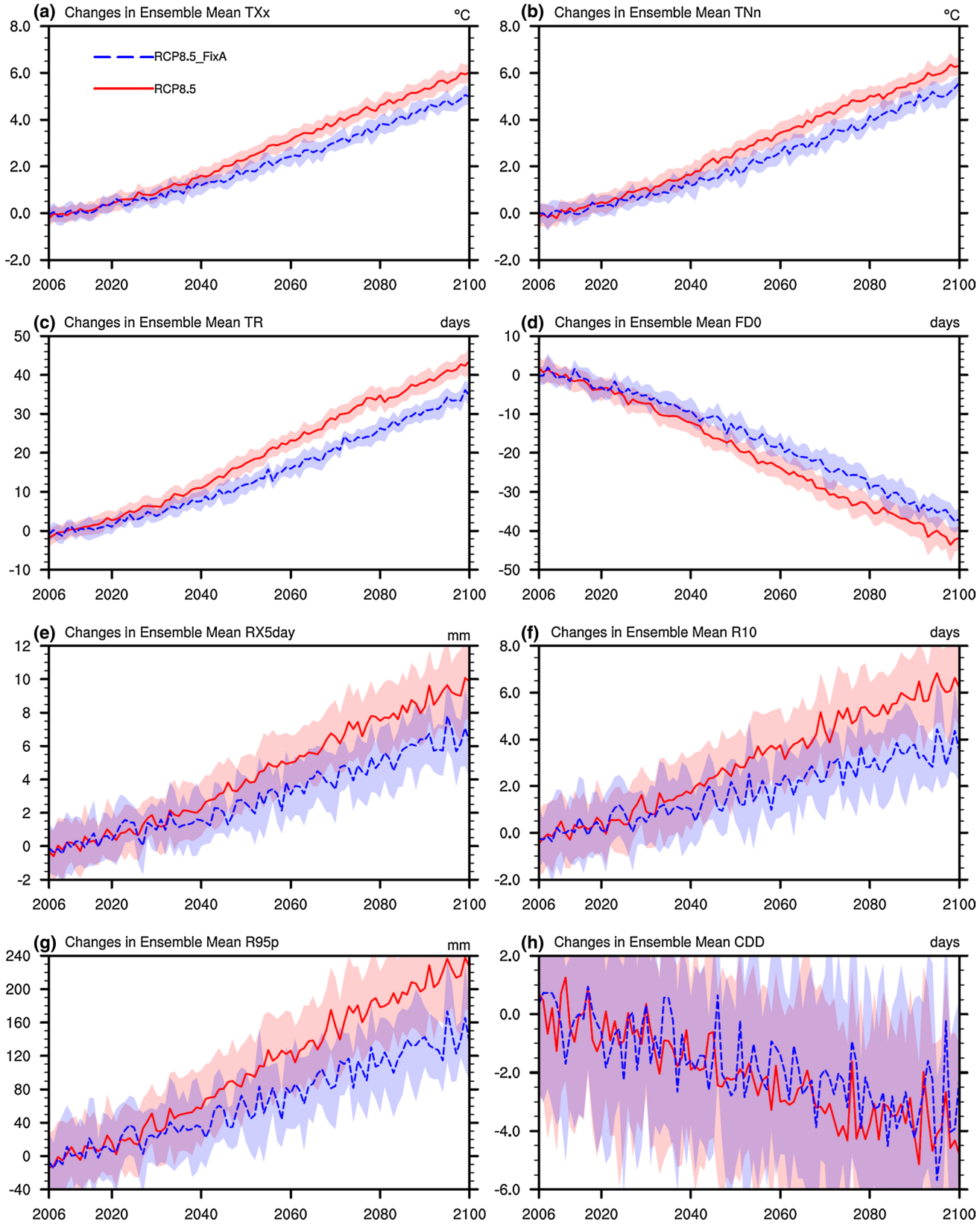

Fig. 3 Time series of changes in annual mean climate extreme indices averaged over China under the RCP8.5 (*red*) and RCP8.5_FixA (*blue*) scenarios from 2006 to 2100 relative to the present day. The *red* and *blue shading* represents two standard deviations from 30 RCP8.5 and 15 RCP8.5_FixA simulations, respectively

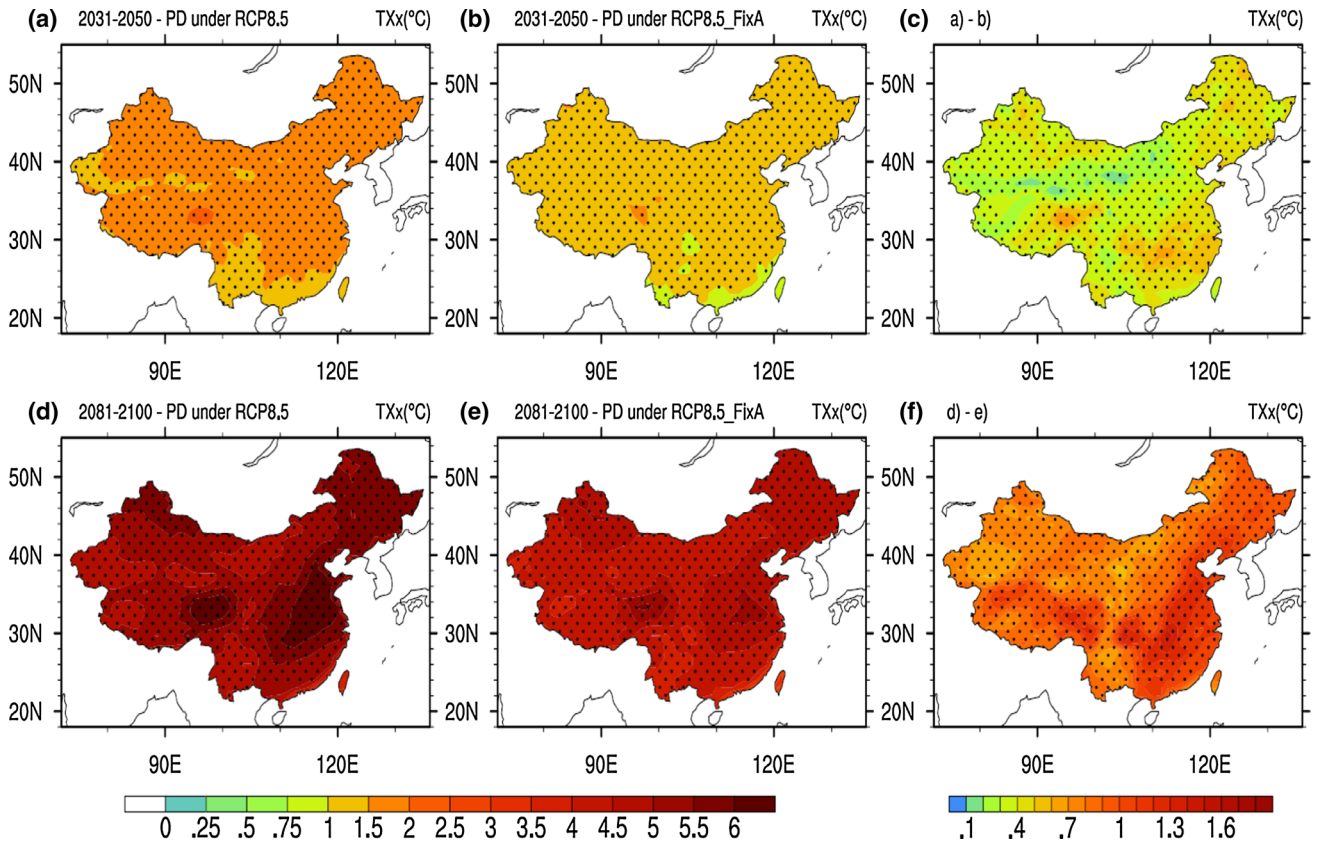

Fig. 4 Changes in maximum of daily max temperature (TXx) over China during the periods **a**, **b** 2031–2050 and **d**, **e** 2081–2100 under the RCP8.5 and RCP8.5_FixA scenarios relative to the PD, respectively (units: °C). **c**, **f** are the contributions of reduced aerosol emissions during the both periods. The *dots* represent significance at ≥95 % confidence level from the *t* test

Table 1 Changes in nationally averaged climate extremes over China during 2031–2050 and 2081–2100 relative to the PD

	2031–2050		2081–2100	
	RCP8.5	RCP8.5_FixA	RCP8.5	RCP8.5_FixA
TXx (°C)	1.6 ± 0.1 (23 ± 8 %)	1.2 ± 0.2	5.3 ± 0.2 (17 ± 3 %)	4.4 ± 0.2
TNn (°C)	1.8 ± 0.2 (27 ± 9 %)	1.3 ± 0.2	5.6 ± 0.2 (16 ± 3 %)	4.8 ± 0.2
TR (days)	11.9 ± 0.9 (31 ± 7 %)	8.2 ± 1.2	38.4 ± 1.0 (20 ± 3 %)	30.9 ± 1.4
FD0 (days)	−13.1 ± 1.0 (25 ± 8 %)	−9.8 ± 1.3	−38.5 ± 1.2 (14 ± 3 %)	−33.1 ± 1.4
RX5 day (mm)	2.6 ± 0.5 (32 ± 20 %)	1.7 ± 0.6	8.7 ± 0.6 (30 ± 6 %)	6.1 ± 0.6
R10 (days)	1.9 ± 0.4 (37 ± 20 %)	1.2 ± 0.5	5.9 ± 0.4 (42 ± 7 %)	3.4 ± 0.5
R95p (mm)	65.0 ± 12.9 (37 ± 20 %)	40.8 ± 15.2	207.9 ± 13.9 (36 ± 7 %)	132.7 ± 14.9
CDD (days)	−1.6 ± 1.1 (11 ± 72 %)	−1.4 ± 0.8	−3.7 ± 1.1 (12 ± 30 %)	−3.2 ± 1.1

The ensemble mean values and standard deviation (numbers following ±) are shown. Values in parentheses are the percentages of changes in climate extremes indices due to reduced aerosol emissions relative to their total changes, i.e., (RCP8.5–RCP8.5_FixA)/RCP8.5

3 Results

3.1 Changes in extreme temperature indices

Figure 4 shows the spatial patterns of changes in TXx over China during 2031–2050 and 2081–2100 under the RCP8.5 and RCP8.5_FixA scenarios relative to the PD, respectively. There are uniform increases in TXx over China during both periods, but the magnitude of increase is larger under the RCP8.5 scenario than the RCP8.5_FixA scenario. This suggests that reduced aerosol emissions will lead to a marked increase in TXx in the future. The increases in TXx

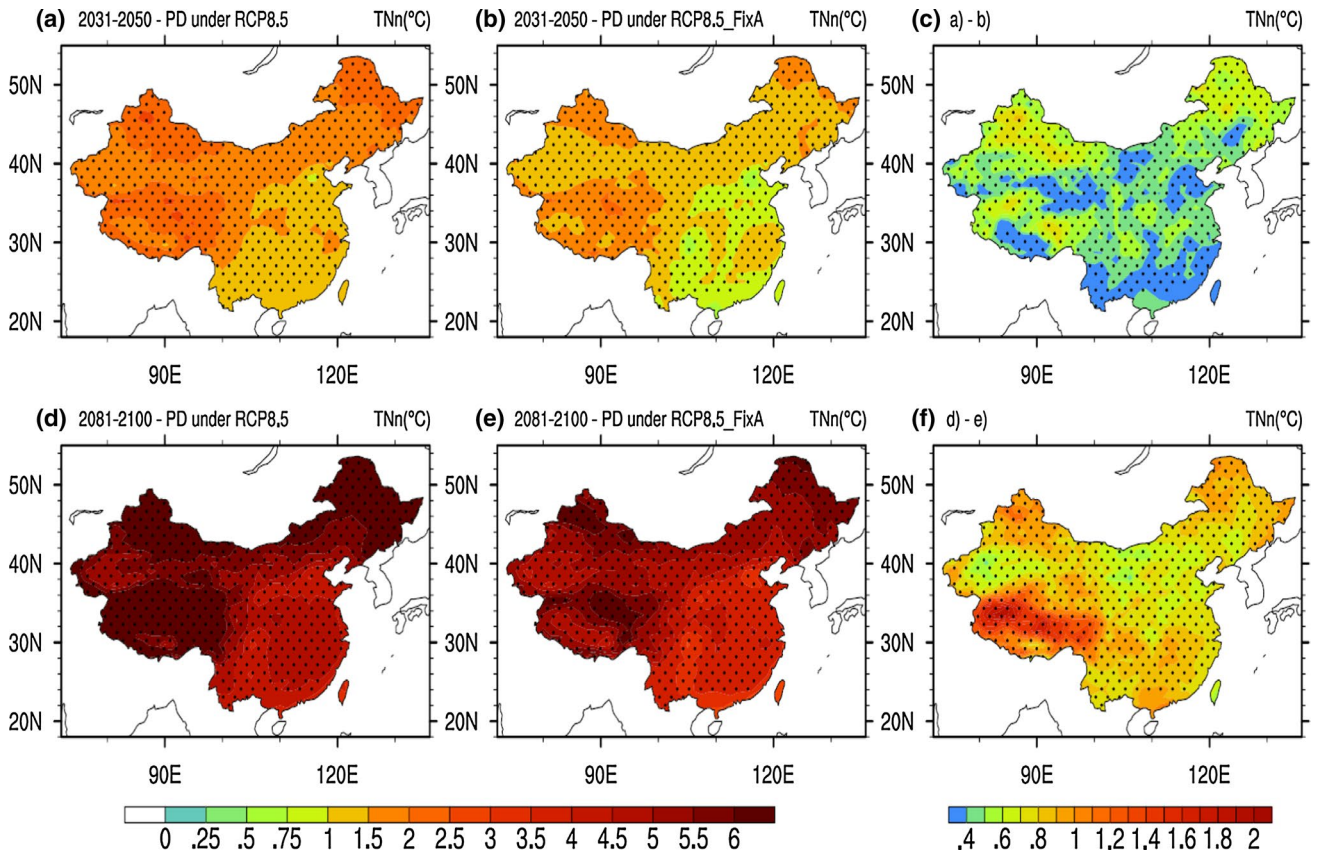

Fig. 5 Same as Fig. 4, but showing changes in minimum of daily min temperature (TNn) over China (units: °C)

during 2031–2050 are generally between 0.75 and 1.5 °C under the RCP8.5_FixA scenario, whereas they range from 1 to 2 °C under the RCP8.5 scenario (Fig. 4a, b). Comparing the RCP8.5 and RCP8.5_FixA scenarios, the decrease in aerosol emissions leads to an additional increase of about 0.4 °C in TXx across most of China during 2031–2050 (Fig. 4c). There are significant spatial variations in the increases in TXx over China during 2081–2100 (Fig. 4d, e). The largest increases are seen over eastern, northeastern, and northwestern China and southern Tibet Plateau (TP), with the maximum being more than 6 °C. Comparing Fig. 4d, e reveals that the continuing reductions in aerosol emissions further magnify the TXx over China, with marked increases found in eastern, southern, and northeastern China and the Sichuan Basin (Fig. 4f). In particular, the aerosol reduction results in an increase of more than 1 °C in TXx over eastern China where the aerosol emissions are large. The projected TXx averaged over China increases by 1.2 ± 0.2 and 4.4 ± 0.2 °C during 2031–2050 and 2081–2100, respectively, under the RCP8.5_FixA scenario, whereas the corresponding values are 1.6 ± 0.1 and 5.3 ± 0.2 °C under the RCP8.5 scenario (Table 1). This suggests that the reduced aerosol emissions contribute to 24 ± 8 and 17 ± 3 % of the total increases in TXx averaged over China during the two periods, respectively, under the RCP8.5 scenario.

Figure 5 shows the projected spatial patterns of changes in TNn over China. The TNn increases during 2031–2050 and 2081–2100 under both scenarios. The increases are larger in western and northern China than eastern and southern China, which is consistent with the results reported by Ji and Kang (2015) using a regional climate model. As with the change in TXx, the increase in TNn is stronger under the RCP8.5 scenario than under the RCP8.5_FixA scenario. The most marked increases in TNn due to the reduced aerosol emissions are seen over the TP and northeastern and northwestern China, with a maximum increase being around 1 °C during 2031–2050 (Fig. 5c) and close to 2 °C during 2081–2100 (Fig. 5f). Figures 3 and 4 show that the spatial patterns of responses in TXx

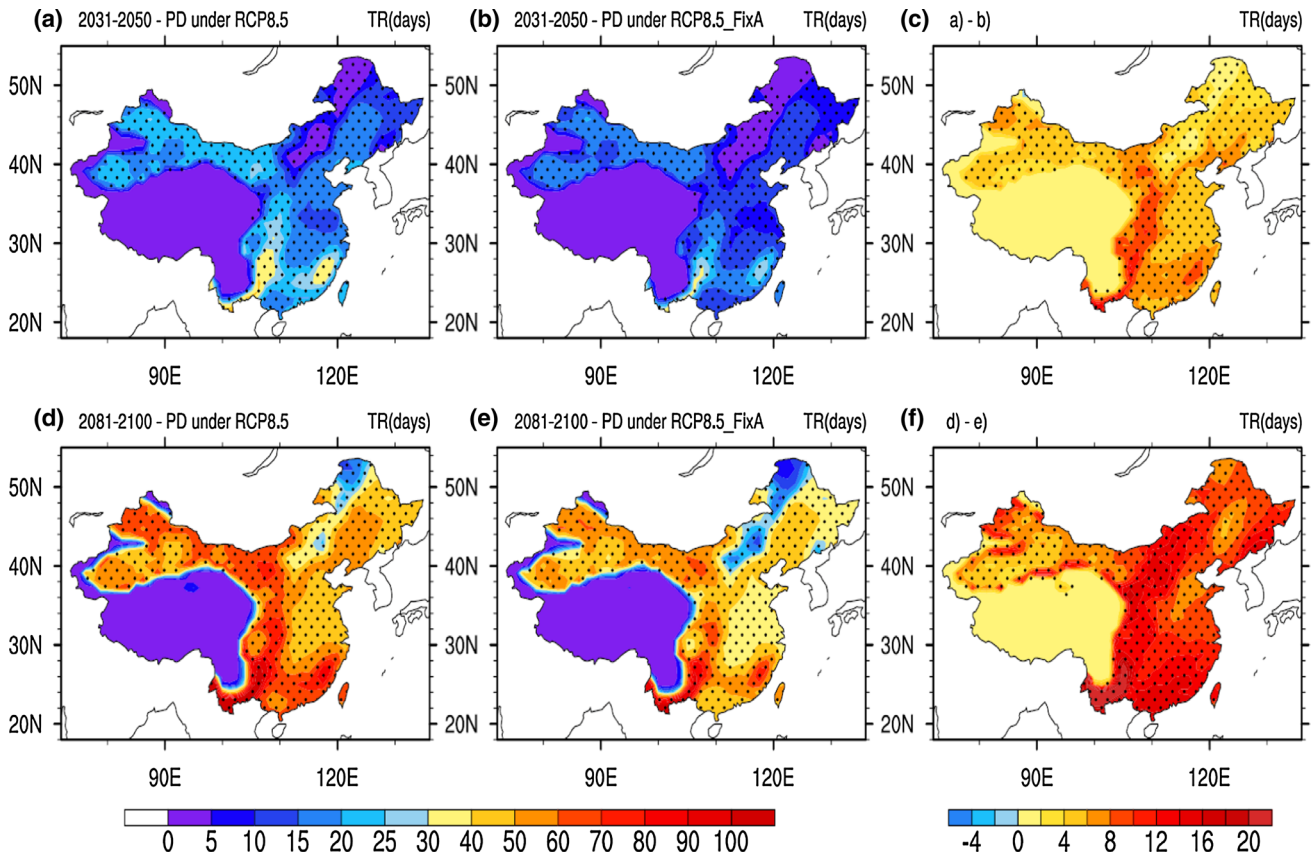

Fig. 6 Same as Fig. 4, but showing changes in tropical nights (TR) over China (units: days)

and TNn are generally similar under the RCP8.5_FixA scenario, whereas they are fairly different under the RCP8.5 scenario. This could be because the TXx occurs at daytime, while the TNn appears at night. However, aerosols directly affect solar radiation at daytime. During the two periods, the reduced aerosol emissions contribute to 27 ± 9 and 16 ± 3 % of the total increases in TNn averaged over China under the RCP8.5 scenario, respectively (Table 1).

Figures 6 and 7 show the projected spatial changes of TR and FD0 over China. Concomitant with the increases in TXx and TNn, the TR also increase over China in the future. The increases are large (>15 days) in most of southwestern, southeastern, and northwestern China during 2031–2050, with a maximum increase >40 days (Fig. 6a, b). The spatial distribution of change in TR during 2081–2100 is similar to that during 2031–2050, but the magnitude is larger, with increases >30 days in most areas of China (Fig. 6d, e). Compared to the GHG-only scenario (RCP8.5_FixA), the aerosol reduction in RCP8.5 significantly increase the TR during 2031–2050, with an increase of >10 days over southwestern China (Fig. 6c), >14 days over southwestern and southern China, and about 10 days over most of northern China during 2081–2100 (Fig. 6f). The increases in TR averaged over China due to the reduced aerosol emissions account for 31 ± 7 and 20 ± 3 % of the total increases during 2031–2050 and 2081–2100 under the RCP8.5 scenario, respectively (Table 1).

The FD0 greatly decreases over China in the future with the rise in surface temperature (Fig. 7). Comparing the differences between the changes in FD0 under the RCP8.5 and RCP8.5_FixA scenarios, the aerosol reduction leads to a decrease in FD0. The largest decreases occur over the TP and central China, with values ranging from 5 to 10 days and 10 to 20 days during 2031–2050 and 2081–2100, respectively. The decreases in FD0 averaged over China due to the reduced aerosol emissions account for 25 ± 8 and 14 ± 3 % of the total decreases during the two periods, respectively (Table 1).

Overall, the aerosol reduction weakens the aerosol net cooling effect, causing an additional warming of the

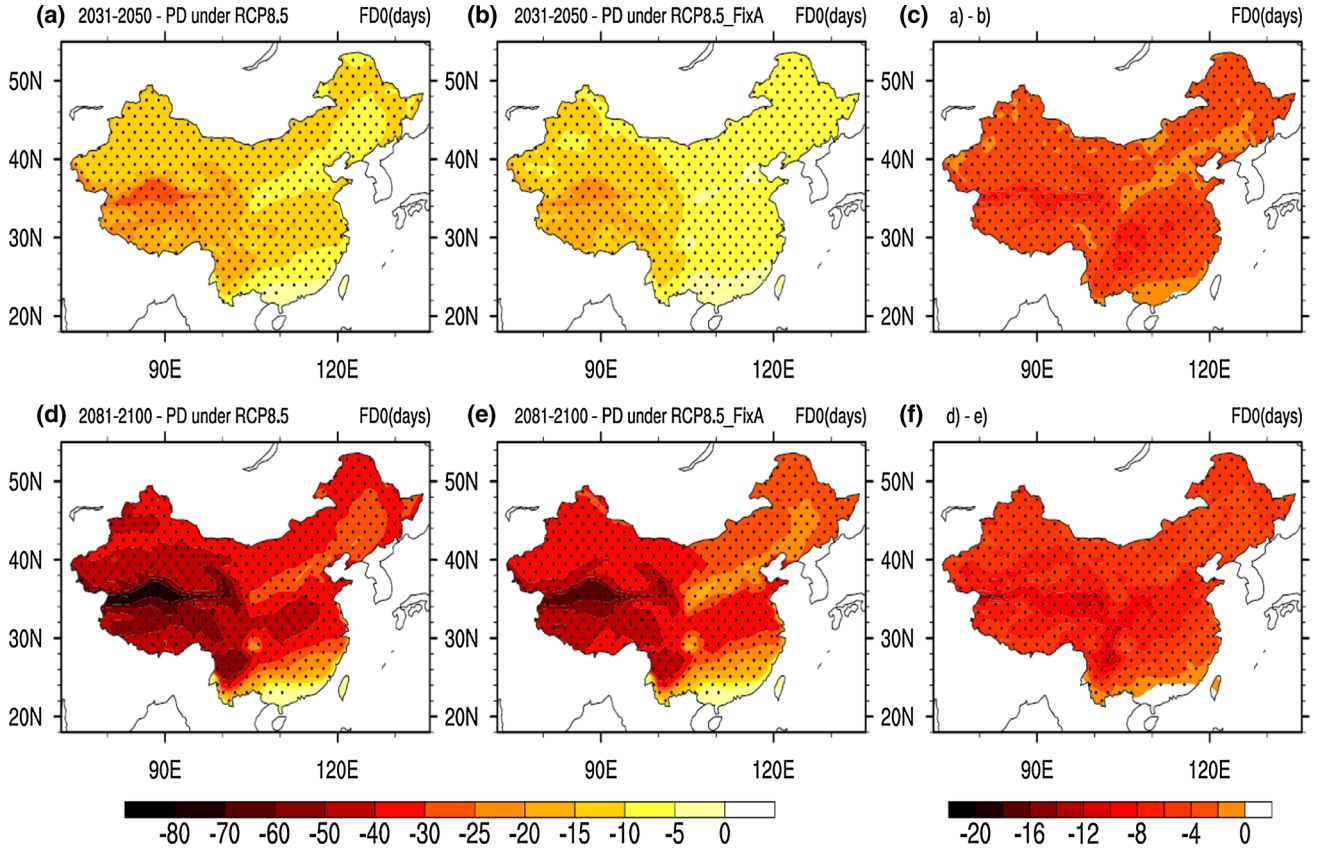

Fig. 7 Same as Fig. 4, but showing changes in frost days (FD0) over China (units: days)

Earth's climate system, thus increasing extreme temperature events. This confirmed the results of previous studies by You et al. (2011) and Caesar and Lowe (2012), which suggested that changes in temperature extremes tended to follow a similar trajectory to the changes in mean temperature.

3.2 Changes in extreme precipitation indices

Figures 8, 9 and 10 display the spatial patterns of changes in RX5 day, R10, and R95p, which represent the wet precipitation extremes, over China during 2031–2050 and 2081–2100 under both scenarios relative to the PD, respectively. Changes in extreme precipitation may generally follow changes in temperature according to the Clausius–Clapeyron equation (Boer 1993; Allen and Ingram 2002; Kharin et al. 2013). The RX5 day increases in the future under both scenarios, and there are similar patterns in the changes in RX5 day over different periods (Fig. 8). The marked increases are located in eastern, southern, and southwestern China, and the Himalayas. Comparing the changes under both scenarios, the reduced aerosol emissions lead to an increase in RX5 day over most of China, with a maximum >14 mm over the Sichuan Basin and southern coast of China. Table 1 shows that the increases in RX5 day averaged over China are 1.7 and 6.1 mm during 2031–2050 and 2081–2100, respectively, under the RCP8.5_FixA scenario, whereas the corresponding increases are 2.6 and 8.7 mm under the RCP8.5 scenario. The aerosol reductions contribute to more than 30 % of the increases in RX5 day averaged over China under the RCP8.5 scenario.

The R10 mostly increases over China in the future (Fig. 9). The largest increase occurs in the Himalayas, southeastern TP, and southern and North China. However, the R10 decreases slightly in some areas of the Shaanxi, Shanxi, Inner Mongolia, and Xinjiang Provinces of China during 2031–2050 and in East China during 2081–2100 under the RCP8.5_FixA scenario, and also decreases in the eastern TP during 2031–2050 under the RCP8.5 scenario. Overall, the reduced aerosol emissions mainly increase the

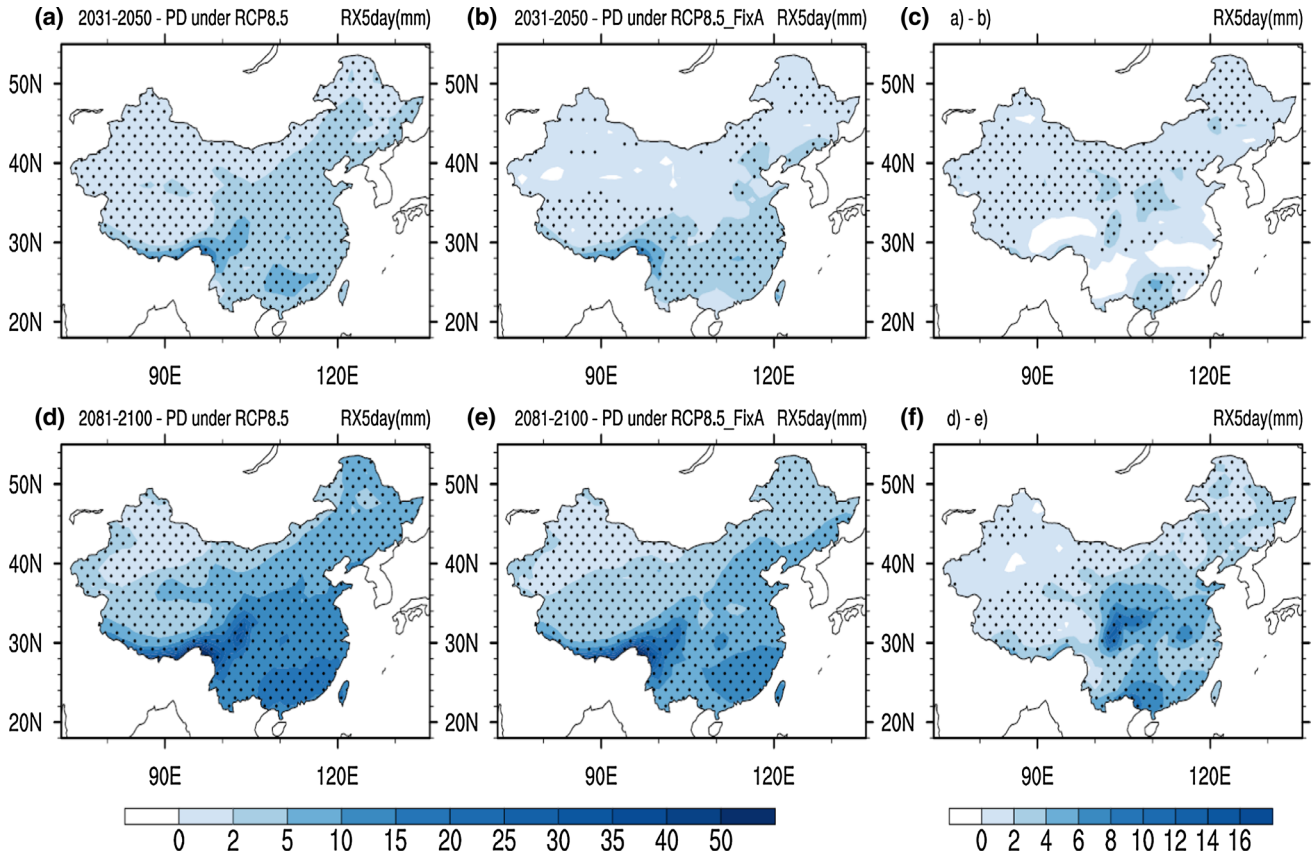

Fig. 8 Same as Fig. 4, but showing changes in max 5-day precipitation amount (RX5 day) over China (units: mm)

R10 over China, especially in the Sichuan Basin and southern China, whereas they lead to a decrease in R10 over the southeastern TP and west of the Hengduan Mountains. The increases in R10 averaged over China due to the aerosol reductions account for 37 ± 20 and 42 ± 7 % of the total increases during 2031–2050 and 2081–2100, respectively (Table 1).

The spatial pattern of change in R95p is generally consistent with that in R10 over China, and is mainly characterized by an increase (Fig. 10). As seen from Fig. 10c, the aerosol reduction increases the R95p in most of China, especially in the Sichuan Basin and southern coast of China, whereas there is a decrease in R95p in some regions of the southeastern TP, west of the Hengduan Mountains, and East China during 2031–2050. Due to the reduced aerosol emissions, the R95p increases over China during 2081–2100, except for the west of the Hengduan Mountains, with the largest increases in the Sichuan Basin and southern coast of China (Fig. 10f). The increases in R95p averaged over China due to the aerosol reduction account for 37 ± 20 and 36 ± 7 % of the total increases during the two periods, respectively (Table 1).

The projected spatial change in CDD, which represents a dry precipitation extreme, is displayed in Fig. 11. Increased total precipitation leads to a decrease in CDD in most regions of China in the future, whereas it causes an increase in CDD over the middle and lower reaches of the Yangtze River, southeastern coast of China, southwestern China, and the eastern TP. Comparing to the 2006–2015, it is found that the occurrence probabilities of low (high) daily rainfall significantly decrease (increase) during 2031–2050 and 2081–2100 under both scenarios (Fig. 12).

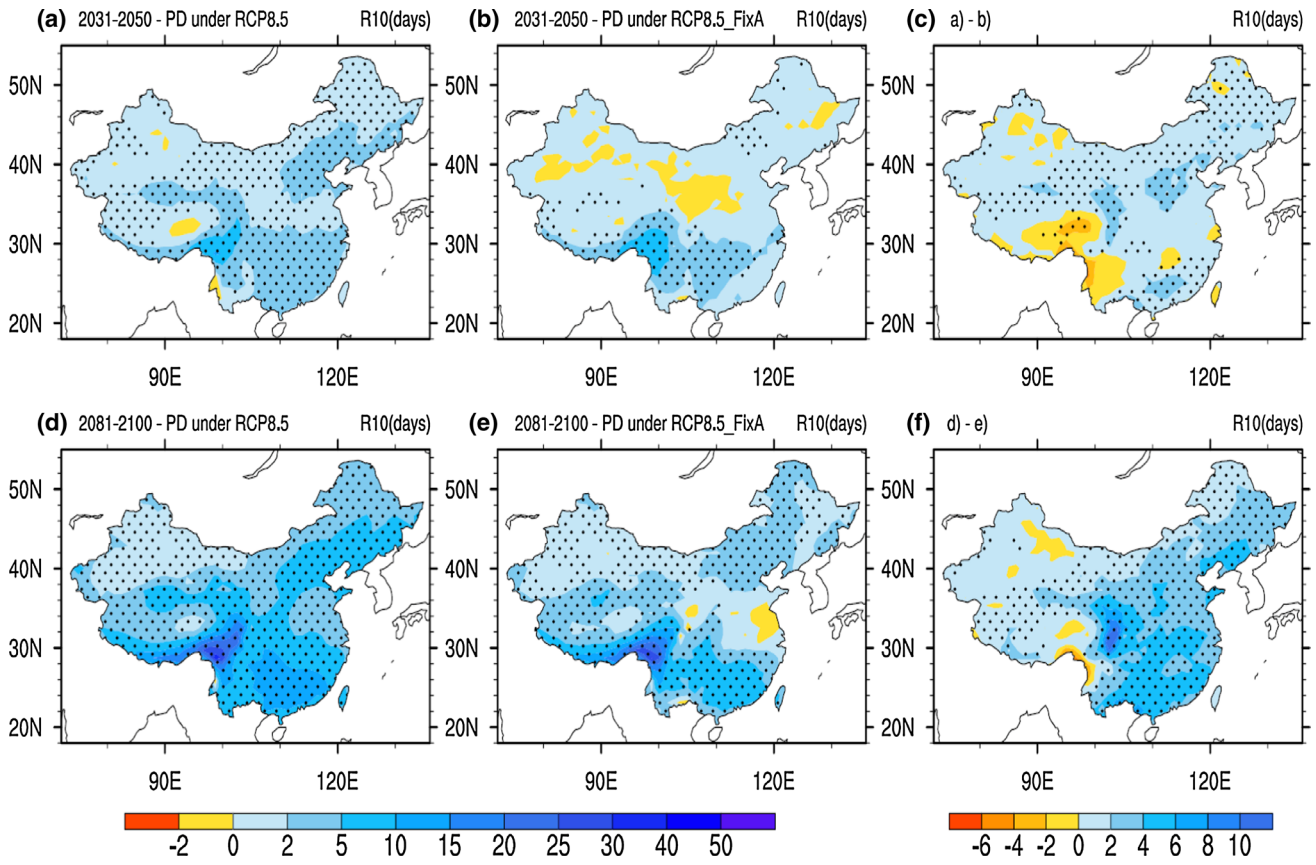

Fig. 9 Same as Fig. 4, but showing changes in number of heavy precipitation days (R10) over China (units: days)

This indicates why both the CDD and extreme precipitation increase in certain regions. As seen from Fig. 11c, the aerosol reduction leads to a decrease of CDD in eastern Xinjiang and western Inner Mongolia, but a marked increase in CDD over the middle and lower reaches of the Yangtze River during 2031–2050. The reduced aerosol emissions decrease the CDD in eastern Xinjiang, Inner Mongolia, and south of the Yangtze River in China, whereas it increases in southwestern Xinjiang, Jiangsu, and Henan Provinces of China and the TP during 2081–2100 (Fig. 11f). The aerosol reduction contributes to 12 % of the total reductions in CDD averaged over China during both periods, respectively (Table 1).

3.3 Normalized changes in climate extremes

Table 2 presents the normalized changes in nationally averaged climate extremes over China scaled by global mean surface temperature changes due to change in aerosols or GHG during 2081–2100 relative to the PD. The motivation for normalization is to understand the differences of changes in climate extremes when giving an equal amount of global warming due to change in GHG or aerosols. The global mean surface air temperatures increase by 1.16 ± 0.06 °C (3.73 ± 0.07 °C) and 0.89 ± 0.07 °C (3.21 ± 0.04 °C) during 2031–2050 (2081–2100) under the RCP8.5 and RCP8.5_FixA scenarios, respectively. When normalized by the global mean surface temperature changes, aerosols have a slightly larger effect on temperature extremes but significantly greater effect on precipitation extremes over China than GHG. This is because aerosols can affect climate through more complex ways (direct, semi-direct, and indirect effects) than GHG. Aerosols can affect climate extremes not only by changing the surface temperature but also by changing the vertical structure of temperature, cloud microphysics, and cloud precipitation (figures not shown). In addition, the aerosol reduction can result in a positive forcing at the top of the atmosphere and negative forcing in the atmosphere relative to the PD (Wang et al. 2015b). This combination of forcings implies a stronger response of hydrological cycle to aerosol reduction relative to GHG (Rotstayn et al. 2013).

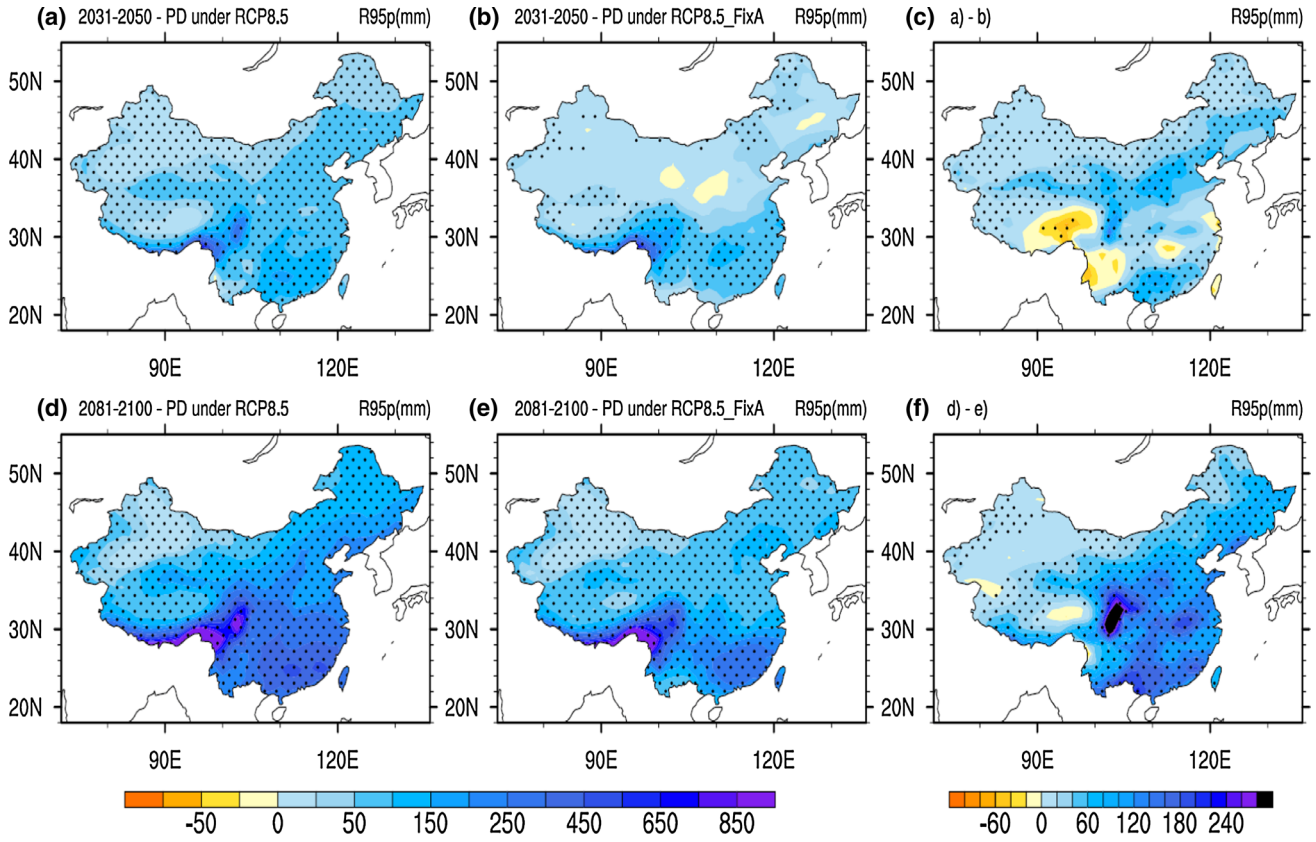

Fig. 10 Same as Fig. 4, but showing changes in very wet days (R95p) over China (units: mm)

4 Discussion and conclusions

Anthropogenic aerosols lead to a variety of adverse effects on the environment and human health. Thus, legislation has been introduced by governments worldwide to reduce the emissions of aerosols and their precursors and improve air quality in recent years (Cofala et al. 2007; Moss et al. 2010). There will be a substantial effect on future climate change due to the aerosol reduction (Rotstayn et al. 2013; Wang et al. 2015b). We explore the effect of reduced aerosol emissions on climate extremes over China under future scenarios by contrasting the projected results from the CESM1 ensemble simulations under the RCP8.5 and RCP8.5 with fixed aerosol emissions scenarios. The projected changes in extreme temperature and precipitation indices over China by CESM1 are generally consistent with previous results (e.g., Sillmann et al. 2013a; Ji and Kang 2015) and observations, although there are differences between the results in some regions.

The aerosol reduction will weaken the aerosol net cooling effect and produce an additional warming of the Earth's climate system (Shindell et al. 2008; Wang et al. 2015a), thus affecting future extreme temperature and precipitation events. Our results show that reduced aerosol emissions will lead to marked increases in TXx, TNn, and TR over China. Relative to the PD, the projected TXx, TNn, and TR averaged over China increase by 1.2 ± 0.2 °C (4.4 ± 0.2 °C), 1.3 ± 0.2 °C (4.8 ± 0.2 °C), and 8.2 ± 1.2 (30.9 ± 1.4) days, respectively, during 2031–2050 (2081–2100) under the RCP8.5_FixA scenario, whereas the corresponding increases are 1.6 ± 0.1 °C (5.3 ± 0.2 °C), 1.8 ± 0.2 °C (5.6 ± 0.2 °C), and 11.9 ± 0.9 (38.4 ± 1.0) days under the RCP8.5 scenario. The small standard deviations of changes in these extreme indices across ensemble members suggest that the results are robust. The spatial distributions show that reduced aerosol emissions result in significant increases in TXx and TNn over northwestern and northeastern China and TR over southwestern China during

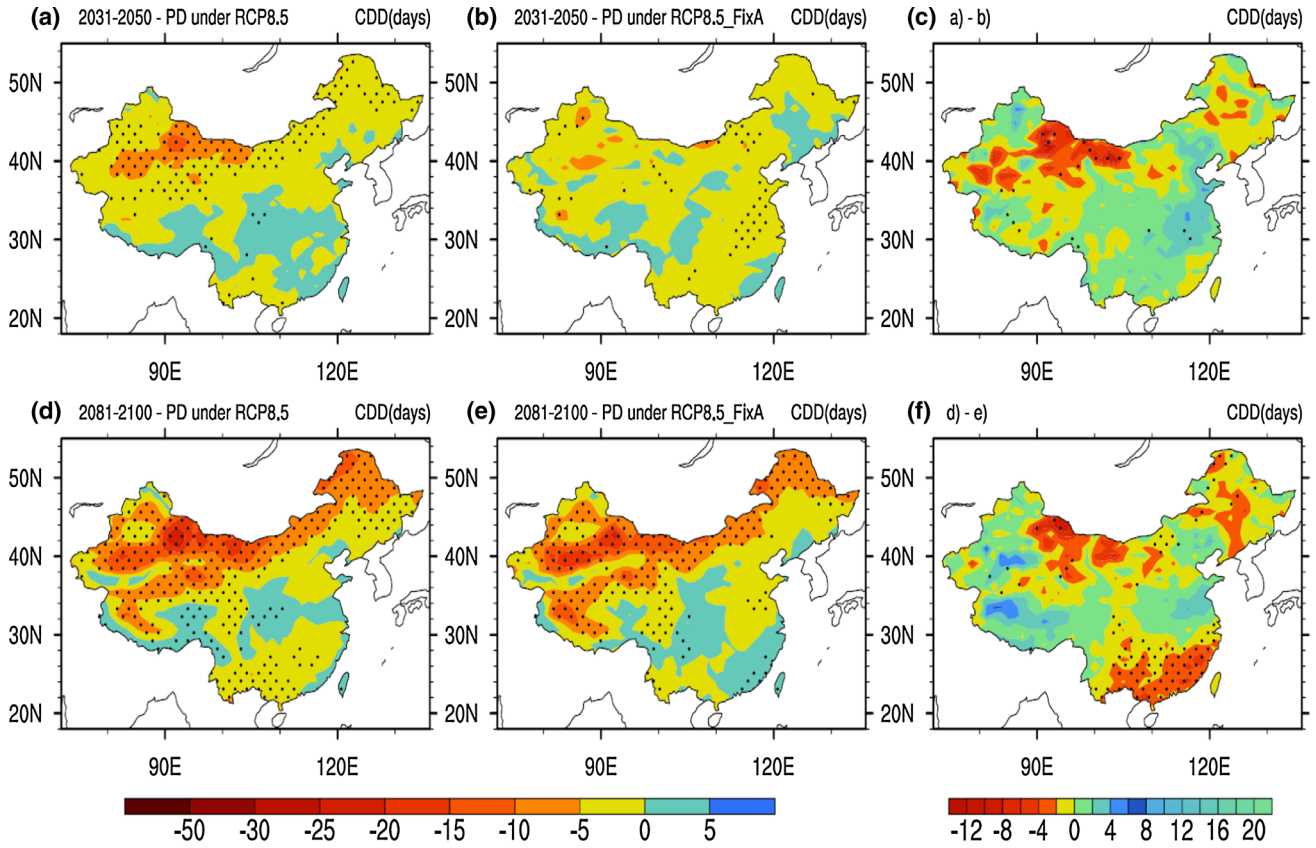

Fig. 11 Same as Fig. 4, but showing changes in consecutive dry days (CDD) over China (units: days)

2031–2050, whereas they lead to marked increases in TXx and TNn over the Sichuan Basin, TP, eastern, northwestern, and northwestern China, and TR over southwestern and southern China during 2081–2100. Moreover, the aerosol reduction decreases the FD0 over China.

Reduced aerosol emissions significantly increase the wet precipitation extremes characterized by different metrics (i.e., RX5 day, R10, and R95p) in China, except for some individual regions. We find large increases in the Sichuan Basin and south of the Yangtze River of China. The aerosol reduction contributes to >30 % of the total increases of all these extreme precipitation indices averaged over China under the RCP8.5 climate change scenario. Moreover, the decreases in CDD due to the reduced aerosol emissions

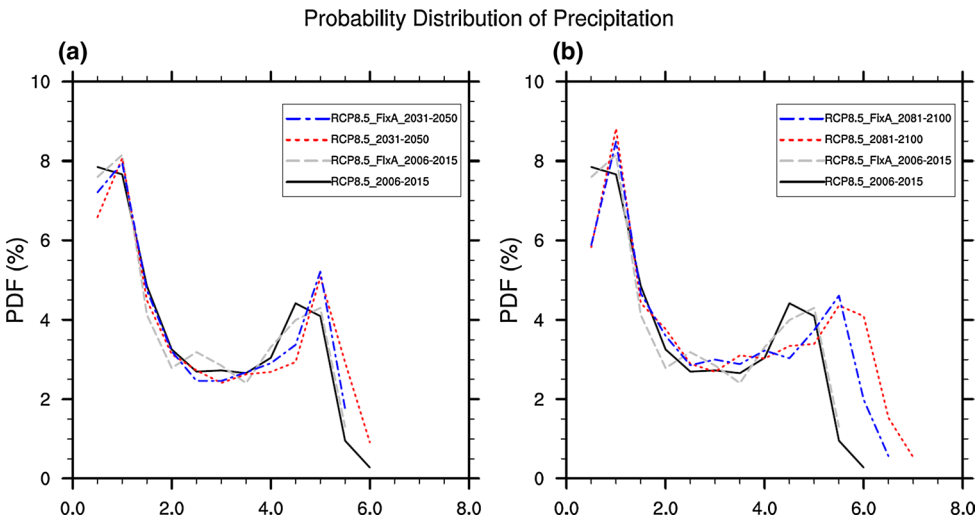

Fig. 12 Probability distribution of daily precipitation over China during the periods 2006–2015, 2031–2050, and 2081–2100 under the RCP8.5 and RCP8.5_FixA scenarios, respectively. The unit of horizontal axis is mm

Table 2 Changes in nationally averaged climate extremes over China due to changes in aerosols (taken as the differences between the RCP8.5 and RCP8.5_FixA simulations during the same period) and GHG, respectively, during 2081–2100 relative to the PD

	Aerosols	GHG
TXx (°C/°C)	1.7 ± 0.2	1.4 ± 0.1
TNn (°C/°C)	1.8 ± 0.3	1.5 ± 0.1
TR (days/°C)	15.2 ± 1.8	9.6 ± 0.4
FD0 (days/°C)	−11.6 ± 1.5	−10.3 ± 0.4
RX5 day (mm/°C)	4.9 ± 1.1	1.9 ± 0.2
R10 (days/°C)	4.4 ± 1.0	1.1 ± 0.2
R95p (mm/°C)	133.3 ± 30.4	41.3 ± 5.1
CDD (days/°C)	−1.7 ± 2.5	−1.0 ± 0.3

All numbers are normalized changes scaled by global mean surface air temperature changes

The ensemble mean values and standard deviation (numbers following ±) are shown

averaged over China, only account for 12 % of their total decreases during both 2031–2050 and 2081–2100.

Aerosols can affect climate through more sophisticated ways relative to GHG. Our results suggest that aerosols have larger effects on temperature and precipitation extremes over China than GHG under an equal amount of global warming due to change in GHG or aerosols. The similar result for heat extremes was reported by Xu et al. (2015). Changes in climate extremes may not be greatest in regions with largest reduction in aerosol emissions. This is because changes in climate extremes are also likely driven by changes in large-scale atmospheric circulation (Haylock and Goodness 2004; Cassou et al. 2005). Wang et al. (2015b) suggested that the future reduction in anthropogenic aerosol emissions would greatly enhance East Asian summer monsoon circulation and precipitation. This may also contribute to the increases in precipitation extremes over China.

Our results are consistent with those reported by Sillmann et al. (2013b), which suggests that the global aerosol reduction will greatly enhance the warming effect due to GHG and lead to significant increases in temperature and precipitation extremes in Europe. Therefore, the reduction of aerosol emissions, which clearly has health benefits, needs to be considered more carefully when devising future emission control strategies at the national and international level.

Acknowledgments The authors thank Andrew Gettelman for his helpful suggestions on the manuscript. This work was supported by the National Natural Science Foundation of China (41575139 and 41305025), Public Meteorology Special Foundation of MOST (GYHY201406023), and MOST (2014BAC16B01). The National Center for Atmospheric Research is supported by the U.S. National Science Foundation.

References

Allen MR, Ingram WJ (2002) Constraints on future changes in climate and the hydrologic cycle. Nature 419:224–232. doi:10.1038/nature01092

Bindoff NL, Stott PA, AchutaRao KM, Allen MR, Gillett N, Gutzler D, Hansingo K, Hegerl G, Hu Y, Jain S, Mokhov II, Overland J, Perlwitz J, Sebbari R, Zhang X (2013) Detection and attribution of climate change: from global to regional. In: Stocker TF, Qin D, Plattner GK, Tignor M, Allen S, Boschung J, Nauels A, Xia Y, Bex V, Midgley P (eds) Climate change 2013: the physical science basis. Contribution of working group I to the fifth assessment report of the Intergovernmental Panel on Climate Change, chap 10. Cambridge University Press, Cambridge

Boer GJ (1993) Climate change and the regulation of the surface moisture and energy budgets. Clim Dyn 8:225–239. doi:10.1007/BF00198617

Boucher O, Randall D, Artaxo P, Bretherton C, Feingold G, Forster P, Kerminen VM, Kondo Y, Liao H, Lohmann U, Rasch P, Satheesh S, Sherwood S, Stevens B, Zhang X (2013) Clouds and aerosols. In: Stocker TF, Qin D, Plattner GK, Tignor M, Allen S, Boschung J, Nauels A, Xia Y, Bex V, Midgley P (eds) Climate change 2013: the physical science basis. Contribution of working group I to the fifth assessment report of the Intergovernmental Panel on Climate Change, chap 7. Cambridge Universtiy Press, Cambridge

Caesar J, Lowe JA (2012) Comparing the impacts of mitigation versus non-intervention scenarios on future temperature and precipitation extremes in the HadGEM2 climate model. J Geophys Res. doi:10.1029/2012JD017762

Cassou C, Terray L, Phillips AS (2005) Tropical Atlantic influence on European heat waves. J Clim 18:2805–2811

Cofala J, Amann M, Klimont Z, Kupiainen K, Hölund-Isaksson L (2007) Scenarios of global anthropogenic emissions of air pollutants and methane until 2030. Atmos Environ 41:8486–8499

Easterling DR, Meehl GA, Parmesan C, Changnon SA, Karl TR, Mearns LO (2000) Climate extremes: observations, modeling, and impacts. Science 289:2068–2074. doi:10.1126/science.289.5487.2068

Fischer EM, Beyerle U, Knutti R (2013) Robust spatially aggregated projections of climate extremes. Nat Clim Change 3:1033–1038. doi:10.1038/nclimate2051

Gettelman A, Liu X, Ghan SJ, Morrison H, Park S, Conley AJ, Klein SA, Boyle J, Mitchell DL, Li J-LF (2010) Global simulations of ice nucleation and ice supersaturation with an improved cloud scheme in the community atmosphere model. J Geophys Res. doi:10.1029/2009JD013797

Ghan SJ, Liu X, Easter RC, Zaveri R, Rasch PJ, Yoon J-H, Eaton B (2012) Toward a minimal representation of aerosols in climate models: comparative decomposition of aerosol direct, semi-direct and indirect radiative forcing. J Clim 25:6461–6476. doi:10.1175/JCLI-D-11-00650.1

Guo L, Highwood EJ, Shaffrey LC, Turner AG (2013) The effect of regional changes in anthropogenic aerosols on rainfall of the East Asian Summer Monsoon. Atmos Chem Phys 13:1521–1534. doi:10.5194/acp-13-1521-2013

Haylock MR, Goodness CM (2004) Inter-annual variability of European extreme winter rainfall and links with mean large-scale circulation. Int J Climatol 24:759–776

Hurrell JW, Holland MM, Gent PR, Ghan S, Kay JE, Kushner PJ, Lamarque J-F, Large WG, Lawrence D, Lindsay K, Lipscomb WH, Long MC, Mahowald N, Marsh DR, Neale RB, Rasch P, Vavrus S, Vertenstein M, Bader D, Collins WD, Hack JJ, Kiehl J, Marshall S (2013) The Community Earth System model: a framework for collaborative research. Bull Am Meteorol Soc 94:1339–1360. doi:10.1175/BAMS-D-12-00121.1

IPCC (2012) Managing the risks of extreme events and disasters to advance climate change adaptation. In: Field CB, Barros V, Stocker TF, Qin D, Dokken DJ, Ebi KL, Mastrandrea MD, Mach KJ, Plattner G-K, Allen SK, Tignor M, Midgley PM (eds) A special report of working groups I and II of the Intergovernmental Panel on Climate Change. Cambridge University Press, Cambridge

Ji Z, Kang S (2015) Evaluation of extreme climate events using a regional climate model for China. Int J Climatol 35:888–902

Jones GS, Stott PA, Christidis N (2008) Human contribution to rapidly increasing frequency of very warm Northern Hemisphere summers. J Geophys Res. doi:10.1029/2007JD008914

Kay JE, Deser C, Phillips A, Mai A, Hannay C, Strand G, Arblaster J, Bates S, Danabasoglu G, Edwards J, Holland M, Kushner P, Lamarque J-F, Lawrence D, Lindsay K, Middleton A, Munoz E, Neale R, Oleson K, Polvani L, Vertenstein M (2014) The Community Earth System Model (CESM1) large ensemble project: a community resource for studying climate change in the presence of internal climate variability. Bull Am Meteorol Soc 96:1333–1349. doi:10.1175/BAMS-D-13-00255.1

Kharin VV, Zwiers FW, Zhang X, Wehner M (2013) Changes in temperature and precipitation extremes in the CMIP5 ensemble. Clim Change 119:345–357. doi:10.1007/s10584-013-0705-8

Lin L, Gettelman A, Xu Y, Fu Q (2015) Simulated differences in 21st century aridity due to different scenarios of greenhouse gases and aerosols. Clim Change (accepted)

Liu X, Easter RC, Ghan SJ, Zaveri R, Rasch P, Shi X, Lamarque J-F, Gettelman A, Morrison H, Vitt F, Conley A, Park S, Neale R, Hannay C, Ekman AML, Hess P, Mahowald N, Collins W, Iacono MJ, Bretherton CS, Flanner MG, Mitchell D (2012) Towards a minimal representation of aerosol direct and indirect effects: model description and evaluation. Geosci Model Dev 5:709–735. doi:10.5194/gmd-4-709-2012

Mascioli NR, Fiore AM, Previdi M, Correa G (2015) Temperature and precipitation extremes in the United States: quantifying the responses to anthropogenic aerosols and greenhouse gases. J Clim. doi: 10.1175/JCLI-D-15-0478.1

Morak S, Hegerl GC, Christidis N (2012) Detectable changes in the frequency of temperature extremes. J Clim 26:1561–1574. doi:10.1175/JCLI-D-11-00678.1

Morrison H, Gettelman A (2008) A new two-moment bulk stratiform cloud microphysics scheme in the Community Atmosphere Model, version 3 (CAM3). Part I: description and numerical tests. J Clim 21(15):3642–3659

Moss RH et al (2010) The next generation of scenarios for climate change research and assessment. Nature 463:747–756. doi:10.1038/nature08823

Myhre G, Shindell D, Bréon FM, Collins W, Fuglestvedt J, Huang J, Koch D, Lamarque JF, Lee D, Mendoza B, Nakajima T, Robock A, Stephens G, Takemura T, Zhang H (2013) Anthropogenic and natural radiative forcing. In: Stocker TF, Qin D, Plattner G-K, Tignor M, Allen SK, Boschung J, Nauels A, Xia Y, Bex V, Midgley PM (eds) Climate change 2013: the physical science basis. Contribution of working group I to the fifth assessment report of the Intergovernmental Panel on Climate Change. Cambridge University Press, Cambridge

Riahi K, Gruebler A, Nakicenovic N (2007) Scenarios of long-term socio-economic and environmental development under climate stabilization. Technol Forecast Soc Chang 74(7):887–935

Rotstayn LD, Collier MA, Chrastansky A, Jeffrey SJ, Luo J-J (2013) Projected effects of declining aerosols in RCP4.5: unmasking global warming? Atmos Chem Phys 13:10883–10905. doi:10.5194/acp-13-10883-2013

Shindell D, Lamarque J-F, Unger N, Koch D, Faluvegi G, Bauer S, Ammann M, Cofala J, Teich H (2008) Climate forcing and air quality change due to regional emissions reductions by economic sector. Atmos Chem Phys 8:7101–7113. doi:10.5194/acp-8-7101-2008

Sillmann J, Roeckner E (2008) Indices for extreme events in projections of anthropogenic climate change. Clim Change 86:83–104. doi:10.1007/s10584-007-9308-6

Sillmann J, Kharin VV, Zwiers FW, Zhang X, Bronaugh D (2013a) Climate extremes indices in the CMIP5 multimodel ensemble: part 2. Future climate projections. J Geophys Res 118:2473–2493. doi:10.1002/jgrd.50188

Sillmann J, Pozzoli L, Vignati E, Kloster S, Feichter J (2013b) Aerosol effect on climate extremes in Europe under different future scenarios. Geophys Res Lett 40:2290–2295. doi:10.1002/grl.50459

Sillmann J, Kharin VV, Zhang X, Zwiers FW, Bronaugh D (2013c) Climate extremes indices in the CMIP5 multimodel ensemble: part 1. Model evaluation in the present climate. J Geophys Res 118:1716–1733. doi:10.1002/jgrd.50203

Stott PA, Jones GS, Christidis N, Zwiers FW, Hegerl G, Shiogama H (2011) Single-step attribution of increasing frequencies of very warm regional temperatures to human influence. Atmos Sci Lett 12(2):220–227. doi:10.1002/asl.315

Sun Y, Zhang X, Zwiers FW, Song L, Wan H, Hu T, Yin H, Ren G (2014) Rapid increase in the risk of extreme summer heat in Eastern China. Nat Clim Change 4:1082–1085. doi:10.1038/nclimate2410

Wang ZL, Zhang H, Zhang XY (2015a) Simultaneous reductions in emissions of black carbon and co-emitted species will weaken the aerosol net cooling effect. Atmos Chem Phys 15:3671–3685. doi:10.5194/acp-15-3671-2015

Wang ZL, Zhang H, Zhang XY (2015b) Projected response of East Asian summer monsoon system to future reductions in emissions of anthropogenic aerosols and their precursors. Clim Dyn. doi:10.1007/s00382-015-2912-7

Wen QH, Zhang X, Xu Y, Wang B (2013) Detecting human influence on extreme temperatures in China. Geophys Res Lett. doi:10.1002/grl.50285

Wu J, Gao XJ (2013) A gridded daily observation dataset over China region and comparison with the other datasets. Chin J Geophys 56:1102–1111

Xu Y, Gao X, Shen Y, Xu C, Shi Y, Giorgi F (2009) A daily temperature dataset over China and its application in validating a RCM simulation. Adv Atmos Sci 26:763–772. doi:10.1007/s00376-009-9029-z

Xu Y, Lamarque J-F, Sanderson B (2015) The importance of aerosol scenarios in projections of future heat extremes. Clim Change. doi:10.1007/s10584-015-1565-1

You QL, Kang SC, Aguilar E, Pepin N, Flugel WA, Yan YP (2011) Changes in daily climate extremes in China and their connection to the large scale atmospheric circulation during 1961–2003. Clim Dyn 36:2399–2417

Zhai P, Zhang X, Wan H, Pan X (2005) Trends in total precipitation and frequency of daily precipitation extremes over China. J Clim 18:1096–1108. doi:10.1175/JCLI-3318.1

Zhang X, Alexander L, Hegerl GC, Jones P, Tank AK, Peterson TC, Trewin B, Zwiers FW (2011) Indices for monitoring changes in extremes based on daily temperature and precipitation data. WIREs Clim Change 2:851–870. doi:10.1002/wcc.147

Zhang H, Wang ZL, Wang ZZ, Liu Q, Gong S, Zhang X-Y, Shen Z, Lu P, Wei X, Che H, Li L (2012) Simulation of direct radiative forcing of typical aerosols and their effects on global climate using an online AGCM-aerosol coupled model system. Clim Dyn 38:1675–1693

Zhou BT, Wen QH, Xu Y, Song L, Zhang X (2014) Projected changes in temperature and precipitation extremes in China by the CMIP5 multimodel ensembles. J Clim 27:6591–6611. doi:10.1175/JCLI-D-13-00761.1